



Published in final edited form as:

*Stem Cell Res.* 2011 May ; 6(3): 215–225. doi:10.1016/j.scr.2011.01.004.

## Serum-deprived human multipotent mesenchymal stromal cells (MSCs) are highly angiogenic

Adam Oskowitz<sup>a</sup>, Harris McFerrin<sup>a</sup>, Miriam Gutschow<sup>a</sup>, Mary Leita Carter<sup>a</sup>, and Radhika Pochampally<sup>a,b,\*</sup>

<sup>a</sup>Center for Gene Therapy, Tulane University Health Science Center, New Orleans, LA 70118, USA

<sup>b</sup>Department of Pharmacology and Tulane Cancer Center, Tulane University Health Science Center, New Orleans, LA 70118, USA

### Abstract

Recent reports have indicated that mesenchymal stromal cells (MSCs) from bone marrow have a potential in vascular remodeling and angiogenesis. Here, we report a unique phenomenon that under serum-deprived conditions MSCs survive and replicate. Secretome analysis of MSCs grown under serum-deprived conditions (SD-MSCs) identified a significant upregulation of pro-survival and angiogenic factors including VEGF-A, ANGPTs, IGF-1, and HGF. An *ex vivo* rat aortic assay demonstrated longer neovascular sprouts generated from rat aortic rings cultured in SD-MSC-conditioned media compared to neovascular sprouts from aortas grown in MSC-conditioned media. With prolonged serum deprivation, a subpopulation of SD-MSCs began to exhibit an endothelial phenotype. This population expressed endothelial-specific proteins including VEGFR2, Tie2/TEK, PECAM/CD31, and eNOS and also demonstrated the ability to uptake acetylated LDL. SD-MSCs also exhibited enhanced microtubule formation in an *in vitro* angiogenesis assay. Modified chick chorioallantoic membrane (CAM) angiogenesis assays showed significantly higher angiogenic potential for SD-MSCs compared to MSCs. Analysis of CAMs grown with SD-MSCs identified human-specific CD31-positive cells in vascular structures. We conclude that under the stress of serum deprivation MSCs are highly angiogenic and a population of these cells has the potential to differentiate into endothelial-like cells.

### Introduction

Mesenchymal stem cells (MSCs) are plastic adherent cells from bone marrow [1,2], referred to in the hematological literature as marrow stromal cells. MSCs were first defined as fibroblastoid colony forming units (CFU-Fs), then as mesenchymal stem/progenitor cells, and most recently as multipotent mesenchymal stromal cells [3]. The angiogenic potential of these cells is an area of current interest. Recent studies have demonstrated a role for MSCs in promoting angiogenesis following tissue injury in several disease models, including myocardial infarction, stroke, hind limb ischemia, and diabetes [4–10]. In addition, MSCs

\*Corresponding author at: Center for Gene Therapy, Tulane University Health Science Center, 1430 Tulane Avenue, SL-99, New Orleans, LA 70118, USA. Fax: +1 504 988 7710. rpo Cham@tulane.edu (R. Pochampally).

have been shown to function as stromal cells in solid tumors [11] and vascular stromal cells in wound healing models [12,13]. The proangiogenic effects of MSCs have been attributed to their ability to secrete cytokines and growth factors that promote endogenous angiogenesis [5-7,9], as well as their ability to contribute directly to angiogenesis through differentiation [6,8,12,13].

One of the properties of stem cells is to survive and support endogenous cells during adverse conditions [14]. *In vitro* studies have demonstrated that MSCs upregulate prosurvival and angiogenic factors, including HGF, IGF-1, and VEGF-A, when exposed to inflammatory cytokines [15]. Studies from our laboratory have demonstrated that complete serum deprivation of MSCs for more than 3 weeks selects a subpopulation of MSCs that are likely primitive uncommitted cells [16]. Accordingly, we set out to test the hypothesis that in response to serum deprivation, MSCs display survival properties characterized by the secretion of prosurvival and angiogenic factors, and that these factors can act in an autocrine, paracrine, or juxtacrine mechanism to enhance angiogenesis.

## Results

### MSCs survive and replicate during serum deprivation

We began by assessing cell proliferation rates of serum-deprived MSCs (SD-MSCs) from two different donors. MSCs were grown to 70% confluence in cell culture media containing serum (CCM) and then the media were replaced with serum-free cell culture media (SF-CCM), containing only amino acids and glucose, creating a nutrient-deprived state. The number of surviving SD-MSCs was determined sequentially over a period of 80 days, at 5 to 10 day intervals (Fig. 1) using trypan blue to exclude dead cells in the total cell count. Initially there was a rapid decrease in the surviving cells soon after cells were placed in SF-CCM. However, around Day 5 of nutrient deprivation the cells began to proliferate again. SD-MSCs continued to proliferate for approximately 30 days. After 30 days, cell numbers remained static, indicating minimal levels of cell replication. The remaining SD-MSCs were able to survive for up to 1 year in SF-CCM.

### SD-MSCs upregulate a variety of angiogenic factors

Next, we hypothesized that in response to serum deprivation, SD-MSCs secrete a number of factors that act in an autocrine manner to support cell growth. Initial cytokine and growth factor immunoblots demonstrated significant expression of prosurvival and angiogenic factors in conditioned media from SD-MSCs (Fig. 2A), while control unconditioned media showed no signal. Microarray assays also indicated upregulation of the receptors for corresponding to specific angiogenic factors such as IGF1 and VEGF-A. Real-time PCR assays demonstrated at least a 2-fold increase in the expression of several angiogenic factors in SD-MSCs from Day 30 of serum deprivation, compared to MSCs that were harvested on Day 0 as described in Pochampally et al. (2004). These factors included the family of angiopoietins (ANGPTs) and VEGF-A (Fig. 2B). In addition, IGF-1 and HGF, two growth factors with proangiogenic activity in ischemic disease models [17,18], showed a greater than 55- and 9-fold increase in SD-MSCs compared to MSCs, respectively (Fig. 2A). ELISAs of conditioned media from SD-MSCs and MSCs confirmed significant increases in

VEGF-A and HGF, and demonstrated a greater than 4-fold increase in levels of angiopoietin (Fig. 2C). IGF-1 levels were below the lowest detectable levels in conditioned media from MSCs, while conditioned media from SD-MSCs contained robust levels of IGF-1 (Fig. 2C).

### **SD-MSCs display an endothelial cell-like phenotype *in vitro***

Real-time PCR assays of SD-MSCs identified that a number of endothelial-specific markers, such as VEGFR2, PECAM/CD31, and VE-cadherin, were expressed in the transcriptome of SD-MSCs but were below detectable levels in MSCs. In addition, the endothelial marker Tie2/TEK was upregulated more than 2-fold in SD-MSCs compared to MSCs (Fig. 3A). Immunocytochemistry confirmed the expression of several of these endothelial markers, as well as eNOS, in a subpopulation of SD-MSCs (Fig. 3B). Next, we sought to determine the origin of the cells exhibiting an endothelial phenotype, to eliminate the possibility of contaminating hematopoietic cells. Flow cytometric analysis demonstrated that SD-MSCs expressed the MSC markers CD90, CD105, CD44, and CD166 and did not contain the hematopoietic markers CD34, CD45, and CD11b [3·14] (Fig. 3C), indicating that SD-MSCs exhibiting an endothelial phenotype are derived from MSCs and not from contaminating hematopoietic cells. Furthermore, approximately 15% of SD-MSCs expressed the endothelial marker Tie2/TEK, while only 1–2% of MSCs expressed this epitope (Fig. 3D). The endothelial cell marker expression preceded tubule formation in the cultures. These experiments were repeated with at least two MSC donor cells that were chosen to represent the preparations that were most and least resistant to serum deprivation (as described in Pochampally, 2004), in triplicates. Secondary antibody only and isotype controls did not show any nonspecific staining (data not shown).

Surprisingly, we observed that with prolonged culture in serum-deprived medium, a population of SD-MSCs formed typical microtubule patterns characteristic of microvessel formation by endothelial cells (Fig. 4A). The structures were cell density dependent with very little tubule formation at lower cell culture densities. In order to substantiate the endothelial phenotype, we tested the ability of SD-MSCs to take up acetylated low-density lipoprotein (ac-LDL), a characteristic of endothelial cells [20]. After 30 days of serum deprivation, a subpopulation of cells displaying a tubular phenotype was able to take up acetylated LDL, while cells with typical MSC morphology (seen in Fig. 4A, Day 30 panel) did not incorporate ac-LDL (Fig. 4B). To determine if the tubule formation seen in SD-MSC cultures was the result of the culture microenvironment or the cells themselves, MSCs and SD-MSCs were plated on grBME at equal density, and tested for tubule formation. The SD-MSCs showed strong tubule formation within the first 24 h of plating, rapidly forming an interconnected tubule network on the entire surface, whereas MSCs showed only a weak tubular potential (Fig. 4C). Using a technique described by Luesch et al. [21], we quantified the degree of tube formation using branch point counting and pattern recognition. SD-MSCs showed significantly more nodes, or connection points, per high-powered field. The number of connections at each node was statistically similar between SD-MSCs and MSCs (Fig. 4D). Interestingly, after 30 days in serum-deprived media 10–20% became spindle shaped and after 80 days of serum deprivation these were the only remaining cells.

### SD-MSCs are highly angiogenic *in vivo*

To test the angiogenic potential of SD-MSCs *in vivo*, we developed a modified version of the chick CAM assay. Plugs of grBME were preincubated with cells and then placed on Day 7 chick CAMs. Following a 7 day incubation, we observed that the angiogenic potential of SD-MSCs was significantly higher than MSCs and the vehicle control (Figs. 5A and B), based on analysis of CAM neovascularization using a traditional 0–4 point scale [19].

In order to test the functional significance of changes in the secretome of SD-MSCs, we investigated the angiogenic potential of conditioned media from MSCs and SD-MSCs using an *ex vivo* rat aortic ring assay [19]. Conditioned medium from MSCs and SD-MSCs from Day 15 of serum deprivation generated significantly longer vascular sprouts from rat aortic rings than unconditioned media (control). The vascular sprouts (measured in micrometers) from aortic rings grown in SD-MSC-conditioned media were also significantly longer than vascular sprouts from MSC-conditioned media (Figs. 6A and 6B). As shown in Fig. 6B the length of sprouts ranged significantly. Interestingly, media from SD-MSCs that had been in a serum-deprived state for 30 days degraded the fibrin clot surrounding the rat aortic rings, making it impossible to assess the angiogenic potential of conditioned media from these cells. These data are consistent with real-time PCR data demonstrating an increase in plasminogen and other proteases in SD-MSCs as compared to MSCs (data not shown). Since many of the proangiogenic growth factors and cytokines appear to continue to increase until Day 30 of serum deprivation, these data likely underestimate the true angiogenic potential of SD-MSCs.

To identify if the neovascular formation contained human cells with endothelial markers, the CAMs were stained with a human-specific antibody to PECAM/CD31. CAMs grown with SD-MSCs demonstrated specific staining for human PECAM/CD31 in areas with morphological characteristics of small vessels. CAMs grown with MSCs showed a smaller number of cells staining positive for PECAM/CD31. There was no cellular staining for human PECAM/CD31 in CAMs grown with vehicle control grBME plugs (Figs. 7A and B), indicating that the observed effect is specific to the SD-MSC phenotype and not variation in cell permeability.

### Discussion

These results demonstrate that subjecting early passage MSCs to serum deprivation for 2–10 weeks selects for a distinct population of cells that have high angiogenic potential. The SD-MSCs were remarkable in that they not only survived complete serum deprivation for prolonged periods of time, but also showed the capacity to proliferate and secrete a significant amount of prosurvival and angiogenic proteins. Interestingly, SD-MSCs exhibit a characteristic biphasic growth curve indicating cell proliferation followed by cell death to stabilize the cell density. This phenotype was observed in more than 5 MSCs donor lines that were cultured using the same culture conditions, controlling for cell density and culture time.

Furthermore, conditioned media from SD-MSCs, and SD-MSCs themselves, had a greater angiogenic potential than MSCs. Several studies indicate that MSCs can reconstitute the

hematopoietic vascular niche *in vivo* when injected into ectopic sites [22·23] and can establish their own microenvironment *in vitro* [24]. Thus, it is not surprising that in the absence of serum, MSCs secrete proteins that promote survival and angiogenesis. Furthermore, conditioned media from MSCs have been shown to have angiogenic potential *in vivo* [9] and affect endothelial survival *in vitro* [25]. Several other studies using ischemic disease models have shown that MSCs promote endogenous angiogenesis via paracrine mechanisms [5·7·9·13]. Specific secreted factors that were upregulated in SD-MSCs, including VEGF-A, HGF, IGF-1, and ANGPTs, have been shown to be important regulators of therapeutic angiogenesis following tissue damage, although not unique to endothelial lineage [18·26·28].

A subset of SD-MSCs also expressed several new proteins expressed by endothelial and hematopoietic cells that were not expressed by control MSCs. However, lack of specific hematopoietic cell marker expression negates the possibility of hematopoietic cell contamination in the cell cultures. Several previous studies have demonstrated that MSCs can differentiate into an endothelial phenotype *in vivo* [8·12·13], and *in vitro* when cultured under low serum conditions with supplemental VEGF [29]. Our data demonstrate, quantitatively, that many of the endothelial markers that are expressed under low serum conditions with exogenous VEGF-A are upregulated in response to serum deprivation. We also demonstrate that these cells lack other hematopoietic markers specifically expressed on hematopoietic cells. This is important as endothelial progenitor cells are believed to express these markers [30] and share a common lineage with hematopoietic cells [31·32]. The spontaneous differentiation of over 80% of surviving SD-MSCs after 80 days into tube-forming cells indicates that a subpopulation of SD-MSCs respond to factors in the medium, and begin to display an endothelial phenotype. Accordingly, we propose a model where MSCs placed under serum-deprived conditions secrete an increased level of pro-survival and angiogenic factors that can act in an autocrine, paracrine, or juxtacrine manner to enhance angiogenesis (Fig. 8).

Our observations support recent interest in using both MSCs and conditioned medium from MSCs to provide therapeutic benefits in pathological vascular conditions including wound repair, ischemic damage, microvascular permeability, and diabetes. In addition, the observations presented here attempt to explain the role of paracrine factors secreted by MSCs in the stromal property of MSCs. This study also has implications in understanding the vasculo-supportive property of MSCs in poorly vascularized injury models such as solid tumors and myocardial infarction models that will have regions that are subjected to serum deprivation.

## Methods

### Cell culture

MSCs from bone marrow aspirates were obtained from the NIH funded National Center for Research Resources (NCRR) Tulane Center for the Preparation and Distribution of Adult Stem Cells at Tulane University. The cells were obtained as frozen vials of passage 1 cells that were shown to be multipotent for differentiation. The cells were negative for hematopoietic markers (CD34, CD36, CD117, and CD45), and positive for CD29 (95%),

CD44 (>93%), CD49c (99%), CD49f (>70%), CD59 (>99%), CD90 (>99%), CD105 (>99%), and CD166 (>99%). All cultures were incubated in complete culture medium (CCM):  $\alpha$ -MEM (GIBCO/BRL; Carlsbad, CA) containing 17% FBS (lot-selected for rapid growth of MSCs; Atlanta Biologicals, Lawrenceville, GA), 100  $\mu$ g/ml streptomycin and 2 or 4 mM L-glutamine (both GIBCO/BRL) at 37 °C with 5% humidified CO<sub>2</sub>, unless otherwise noted. Serum-deprived MSCs were prepared by growing Passage 1 or 2 MSCs seeded at 1000 cells/cm<sup>2</sup> to 70–80% confluence and replacing the CCM with  $\alpha$ -MEM containing 100  $\mu$ g/ml streptomycin (SF-CCM). Media were subsequently changed every 3 days. The cells are harvested with trypsin/EDTA and counted after trypan blue exclusion of dead cells. All the experiments were performed with 2–5 donors that represent the most and least serum-deprivation-resistant MSCs donors.

### Immunoblots

For collection of conditioned media, SD-MSCs were washed three times in PBS to remove nonadherent cells and debris, and then incubated in fresh SF-CCM for a period of 24 h. The conditioned media were collected and filtered to remove any cellular components. Fresh conditioned media were then tested for the presence of specific proteins using the Human Angiogenesis Antibody array (RayBiotech, Inc.; Norcross, GA) according to the manufacturer's protocol. As control unconditioned media were used and no signal was seen on the blot.

### Real-time PCR

Total RNA was extracted from MSCs or SD-MSCs using the RNeasy Mini Kit (Qiagen; Valencia CA), and 500 ng was converted into cDNA with the RT2 First Strand Kit (SuperArray Bioscience Corp.; Frederick, MD). Real-time PCR was performed using the RT2 Angiogenesis PCR array with the RT2 SYBR Green Master Mix (both SuperArray Bioscience Corp.) according to the manufacturer's protocol. PCR arrays were run with an ABI PRISM 7900HT Sequence Detection System (Applied Biosystems; Foster City, CA) using the SDS 2.2 program. Fold change in transcript levels were calculated using the  $C_t$  method of relative quantification, by normalizing samples to the average of 5 endogenous controls ( $\beta$ -2-microglobulin,  $\beta$ -actin, GAPDH, ribosomal protein L13a, hypoxanthine phosphoribosyltransferase-1) and subsequently comparing SD-MSC samples to MSC samples. Samples amplifying at a  $C_t$  value greater than 35 were considered below the detectable range and the value of 35 was used for fold change calculations.

### Immunocytochemistry

For immunofluorescence microscopy, cells grown on chamber slides were washed in PBS and fixed in phosphate-buffered 4% (v/v) paraformaldehyde for 15 min. Mouse anti-human CD31/PECAM (Clone P2B1; Abcam; Cambridge, MA), mouse anti-Tie 2 (Clone 83715; R&D Biosystems; Minneapolis, MN) rabbit anti-VEGFR2, or rabbit anti-eNOS (both Abcam) were used as primary antibodies, and goat anti-mouse IgG or goat anti-rabbit IgG conjugated to AlexaFluor488 or AlexaFluor594 (Molecular Probes; Carlsbad, Ca) were used as secondary antibodies. Appropriate controls to include isotypes and secondary only were used in parallel experiments. Images were acquired on an upright epifluorescent spinning

disk confocal microscope (Hamamatsu EM-CCD C9100; Hamamatsu City, Japan) using StereoInvestigator software (MBF Bioscience, Williston, VT).

### Fluorescence-activated cell scanning

Approximately 200,000 MSCs or SD-MSCs were lifted with trypsin/EDTA (0.25% Trypsin/1 mM EDTA; GIBCO/BRL) for 5 min at 37 °C. Trypsin was then inactivated by adding an equal volume of FBS and the cells were concentrated by centrifugation at 500 *g* for 5 min and resuspended in 200  $\mu$ l of PBS containing the appropriate fluorescently conjugated antibody. The following mouse monoclonal antibodies were used: CD34 (Clone 581), CD45 (Clone J33), CD11b (Clone Bear1), CD44 (Clone G44-26), CD166 (Clone 3A6), CD90 (Clone Thy1/310), CD105 (Clone IG2) (all Beckman Coulter; Miami, FL), and Tie2 (Clone 83715; R&D Systems). After a 20 min incubation period cells were washed 3 times in PBS and assayed by FACScanning (Cytomics FC 500; Beckman Coulter). All the experiments were performed in triplicates and repeated with two or more MSC donors.

### *In vitro* angiogenesis assay

MSCs or SD-MSCs were lifted with trypsin/EDTA (0.25% trypsin/1 mM EDTA; GIBCO/BRL) for 5 min at 37 °C. Trypsin was then inactivated by adding an equal volume of FBS. The cells were concentrated by centrifugation at 500 *g* for 5 min, resuspended in 200  $\mu$ l of PBS, and replated on growth factor-reduced basement membrane extract (grBME), also called Matrigel (R&D Systems, <http://www.rndsystems.com/products.aspx>) at 25 000 cell/cm<sup>2</sup> and cultured for 24 h. Images were acquired on an upright spinning disk confocal microscope (Hamamatsu EM-CCD C9100) using StereoInvestigator software (MBF Bioscience). Tube formation was assessed blindly based on total number of nodes/100 $\times$  field and branch points/node.

### Rat aortic ring assay

For collection of conditioned media, MSCs or SD-MSCs were washed three times in PBS to remove nonadherent cells and debris and then incubated in fresh SF-CCM for a period of 24 h. The conditioned media were collected and filtered to remove any cellular components and were concentrated approximately 20-fold using a stirred cell with a 1-kDa molecular weight cutoff ultrafiltration disk (both Millipore; Billerica, MA). Samples were then normalized to total protein content using the BCA Protein Assay for total protein quantitation (Pierce; Rockford, IL). Nonconcentrated media had undetectable levels of protein. Paragon Biosystems performed the rat aortic ring assay using their standard protocol (Baltimore, MD). Briefly, aortic rings from Wistar rats (1–2 months) were harvested, embedded in fibrin clots, and placed in 24-well plates. The rings were then incubated in conditioned media from SD-MSCs or MSCs supplemented with 1% FBS or a vehicle control supplemented with 1% FBS. Six aortic rings were used for each experimental group as well as the vehicle control. Media were changed every 48 h. After an incubation period of 10 days the aortic rings were fixed with phosphate-buffered 10% (v/v) formalin solution. Blinded microscopic evaluations of the fixed rings were performed using an Olympus IX-70 inverted microscope at 4 $\times$  bright-field magnification. Ten random measurements were made per half of each ring. Each measurement reflected the radial length of one sprout in micrometers as determined by computer-assisted image analysis. Digital images were generated using a Retiga 2000R

digital camera (QImaging, Burnaby, BC). Image analysis was performed using Image-Pro Plus 5.1 (Media Cybernetics Inc., Silver Spring, MD).

### Chick CAM assay

Fertilized white leghorn chick embryos were obtained from Charles River Laboratories (Wilmington, MA). Following 2 days of incubation in a 39 °C humidified incubator with rocking, eggs were swabbed with 70% ethanol, and 2 ml of albumin was withdrawn from the smaller end of the egg with an 18-gauge needle. Two days later, the air pocket in the larger end of the egg was ruptured with a 21-gauge needle, and a window was cut in the side of the egg with a Dremel tool to expose the chorioallantoic membrane (CAM). The window was then resealed with tape. On Day 7 of incubation grBME (R&D Systems) plugs with equal numbers of (0.2 to 2 million) SD-MSCs, MSCs or vehicle control were added through the window and the window was resealed with tape. After 7 additional days of incubation (E15), the window was enlarged, and digital images of the CAM were taken with a MiniVid digital camera (LW Scientific, Lawrenceville, GA) and scored blindly on a scale of 0–4 for angiogenesis.

### Immunohistochemistry

For immunofluorescence microscopy, the area of the CAM surrounding the plug was excised, embedded in Tissue-Tek OCT mounting medium (Sakura; Zoeterwoude, The Netherlands), frozen, and sectioned. Mouse anti-human CD31/PECAM1gG (Clone P2B1: Abcam) was used at a dilution of 1:100, and goat anti-mouse IgG AlexaFluor488 (Molecular Probes) was used at 2 µg/ml. Images were acquired on an upright spinning disk confocal microscope (Hamamatsu EM-CCD C9100) using StereoInvestigator software (MBF Bioscience).

### Statistical analysis

Statistical analysis was performed using Microsoft Excel and with the help of Analyse-it statistical analysis plug-in software (Analyse-it Software, Ltd), when necessary. All *P* values noted were determined using a two-sample method Student's *t* test, assuming unequal variances, with *P* values generated for two tails. Sample size and specific *P* values are noted in the figure legends. Confidence intervals were generated using Dunnett's test for comparison of samples to control.

### Acknowledgments

Some of the materials employed in this work were provided by the Tulane Center for Gene Therapy through a grant from NCRR of the NIH, Grant P40RR017447 and Grants NIH AR 47796 and AR 48323, the Oberkotter Foundation, the HCA the Health Care Company, and the Louisiana Gene Therapy Research Consortium to Dr. Darwin J. Prockop. We also thank Mr. Patrice Penfornis for technical assistance and Margaret Wolf for critical review of the manuscript.

### Abbreviations

<b>MSC</b>	mesenchymal stem cell
<b>SD-MSC</b>	serum-deprived mesenchymal stem cell



<b>acLDL</b>	acetylated low-density lipoprotein
<b>grBME</b>	growth factor reduced basement membrane extract
<b>CAM</b>	chorioallantoic membrane
<b>FBS</b>	fetal bovine serum
<b>CCM</b>	cell culture media containing serum
<b>SF-CCM</b>	serum-free cell culture media

## References

1. Prockop DJ. Marrow stromal cells as stem cells for nonhematopoietic tissues. *Science*. 1997; 276:71–74. [PubMed: 9082988]
2. Owen M, Friedenstein AJ. Stromal stem cells: marrow-derived osteogenic precursors. *Ciba Found. Symp.* 1988; 136:42–60. [PubMed: 3068016]
3. Dominici M, et al. Minimal criteria for defining multipotent mesenchymal stromal cells. The International Society for Cellular Therapy position statement 3. *Cytotherapy*. 2006; 8:315–317. [PubMed: 16923606]
4. Kocher AA, et al. Neovascularization of ischemic myocardium by human bone-marrow-derived angioblasts prevents cardiomyocyte apoptosis, reduces remodeling and improves cardiac function. *Nat. Med.* 2001; 7:430–436. [PubMed: 11283669]
5. Kinnaird T, et al. Local delivery of marrow-derived stromal cells augments collateral perfusion through paracrine mechanisms. *Circulation*. 2004; 109:1543–1549. [PubMed: 15023891]
6. Iwase T, et al. Comparison of angiogenic potency between mesenchymal stem cells and mononuclear cells in a rat model of hindlimb ischemia. *Cardiovasc. Res.* 2005; 66:543–551. [PubMed: 15914119]
7. Al-Khalidi A, Al-Sabti H, Galipeau J, Lachapelle K. Therapeutic angiogenesis using autologous bone marrow stromal cells: improved blood flow in a chronic limb ischemia model. *Ann. Thorac. Surg.* 2003; 75:204–209. [PubMed: 12537217]
8. Lee RH, et al. Multipotent stromal cells from human marrow home to and promote repair of pancreatic islets and renal glomeruli in diabetic NOD/scid mice. *Proc. Natl Acad. Sci. USA*. 2006; 103:17438–17443. [PubMed: 17088535]
9. Gnecci M, et al. Paracrine action accounts for marked protection of ischemic heart by Akt-modified mesenchymal stem cells. *Nat. Med.* 2005; 11:367–368. [PubMed: 15812508]
10. Chopp M, Li Y. Treatment of neural injury with marrow stromal cells. *Lancet Neurol*. 2002; 1:92–100. [PubMed: 12849513]
11. Karnoub AE, et al. Mesenchymal stem cells within tumour stroma promote breast cancer metastasis. *Nature*. 2007; 449:557–563. [PubMed: 17914389]
12. Wu Y, Chen L, Scott PG, Tredget EE. Mesenchymal stem cells enhance wound healing through differentiation and angiogenesis. *Stem Cells*. 2007; 25:2648–2659. [PubMed: 17615264]
13. Sasaki M, et al. Mesenchymal stem cells are recruited into wounded skin and contribute to wound repair by transdifferentiation into multiple skin cell type. *J. Immunol.* 2008; 180:2581–2587. [PubMed: 18250469]
14. Phinney DG, Prockop DJ. Concise review. Mesenchymal stem/multipotent stromal cells: the state of transdifferentiation and modes of tissue repair—current views. *Stem Cells*. 2007; 25:2896–2902. [PubMed: 17901396]
15. Wang M, Crisostomo PR, Herring C, Meldrum KK, Meldrum DR. Human progenitor cells from bone marrow or adipose tissue produce VEGF, HGF, and IGF-I in response to TNF by a p38 MAPK-dependent mechanism. *Am. J. Physiol. Regul. Integr. Comp. Physiol.* 2006; 291:R880–R884. [PubMed: 16728464]

16. Pochampally RR, Smith JR, Ylostalo J, Prockop DJ. Serum deprivation of human marrow stromal cells (hMSCs) selects for a subpopulation of early progenitor cells with enhanced expression of OCT-4 and other embryonic genes. *Blood*. 2004; 103:1647–1652. [PubMed: 14630823]
17. Aoki M, et al. Angiogenesis induced by hepatocyte growth factor in non-infarcted myocardium and infarcted myocardium: up-regulation of essential transcription factor for angiogenesis, ets. *Gene Ther*. 2000; 7:417–427. [PubMed: 10694824]
18. Urbanek K, et al. Cardiac stem cells possess growth factor-receptor systems that after activation regenerate the infarcted myocardium, improving ventricular function and long-term survival. *Circ. Res*. 2005; 97:663–673. [PubMed: 16141414]
19. Auerbach R, Lewis R, Shinnars B, Kubai L, Akhtar N. Angiogenesis assays: a critical overview. *Clin. Chem*. 2003; 49:32–40. [PubMed: 12507958]
20. Voyta JC, Via DP, Butterfield CE, Zetter BR. Identification and isolation of endothelial cells based on their increased uptake of acetylated-low density lipoprotein. *J. Cell Biol*. 1984; 99:2034–2040. [PubMed: 6501412]
21. Luesch H, et al. A functional genomics approach to the mode of action of apratoxin A. *Nat. Chem. Biol*. 2006; 2:158–167. [PubMed: 16474387]
22. Sacchetti B, et al. Self-renewing osteoprogenitors in bone marrow sinusoids can organize a hematopoietic microenvironment. *Cell*. 2007; 131:324–336. [PubMed: 17956733]
23. Bianco P, Robey PG. Stem cells in tissue engineering. *Nature*. 2001; 414:118–121. [PubMed: 11689957]
24. Ylostalo J, Bazhanov N, Prockop DJ. Reversible commitment to differentiation by human multipotent mesenchymal stem cells (MSCs) in single-cell derived colonies. *Exp. Hematol*. 2008; 36(10):1390–1402. [PubMed: 18619725]
25. Hung SC, Pochampally RR, Chen SC, Hsu SC, Prockop DJ. Angiogenic effects of human multipotent stromal cell conditioned medium activate the PI3K-Akt pathway in hypoxic endothelial cells to inhibit apoptosis, increase survival, and stimulate angiogenesis. *Stem Cells*. 2007; 25:2363–2370. [PubMed: 17540857]
26. Sadat S, et al. The cardioprotective effect of mesenchymal stem cells is mediated by IGF-I and VEGF. *Biochem. Biophys. Res. Commun*. 2007; 363:674–679. [PubMed: 17904522]
27. Matsumoto R, et al. Vascular endothelial growth factor-expressing mesenchymal stem cell transplantation for the treatment of acute myocardial infarction. *Arterioscler. Thromb. Vasc. Biol*. 2005; 25:1168–1173. [PubMed: 15831811]
28. Shim WS, et al. Angiopoietin-1 promotes functional neovascularization that relieves ischemia by improving regional reperfusion in a swine chronic myocardial ischemia model. *J. Biomed. Sci*. 2006; 13:579–591. [PubMed: 16547766]
29. Oswald J, et al. Mesenchymal stem cells can be differentiated into endothelial cells in vitro. *Stem Cells*. 2004; 22:377–384. [PubMed: 15153614]
30. Asahara T, et al. Isolation of putative progenitor endothelial cells for angiogenesis. *Science*. 1997; 275:964–967. [PubMed: 9020076]
31. Kabrun N, et al. Flk-1 expression defines a population of early embryonic hematopoietic precursors. *Development*. 1997; 124:2039–2048. [PubMed: 9169850]
32. Nishikawa SI, Nishikawa S, Hirashima M, Matsuyoshi N, Kodama H. Progressive lineage analysis by cell sorting and culture identifies FLK1 + VE-cadherin + cells at a diverging point of endothelial and hemopoietic lineages. *Development*. 1998; 125:1747–1757. [PubMed: 9521912]

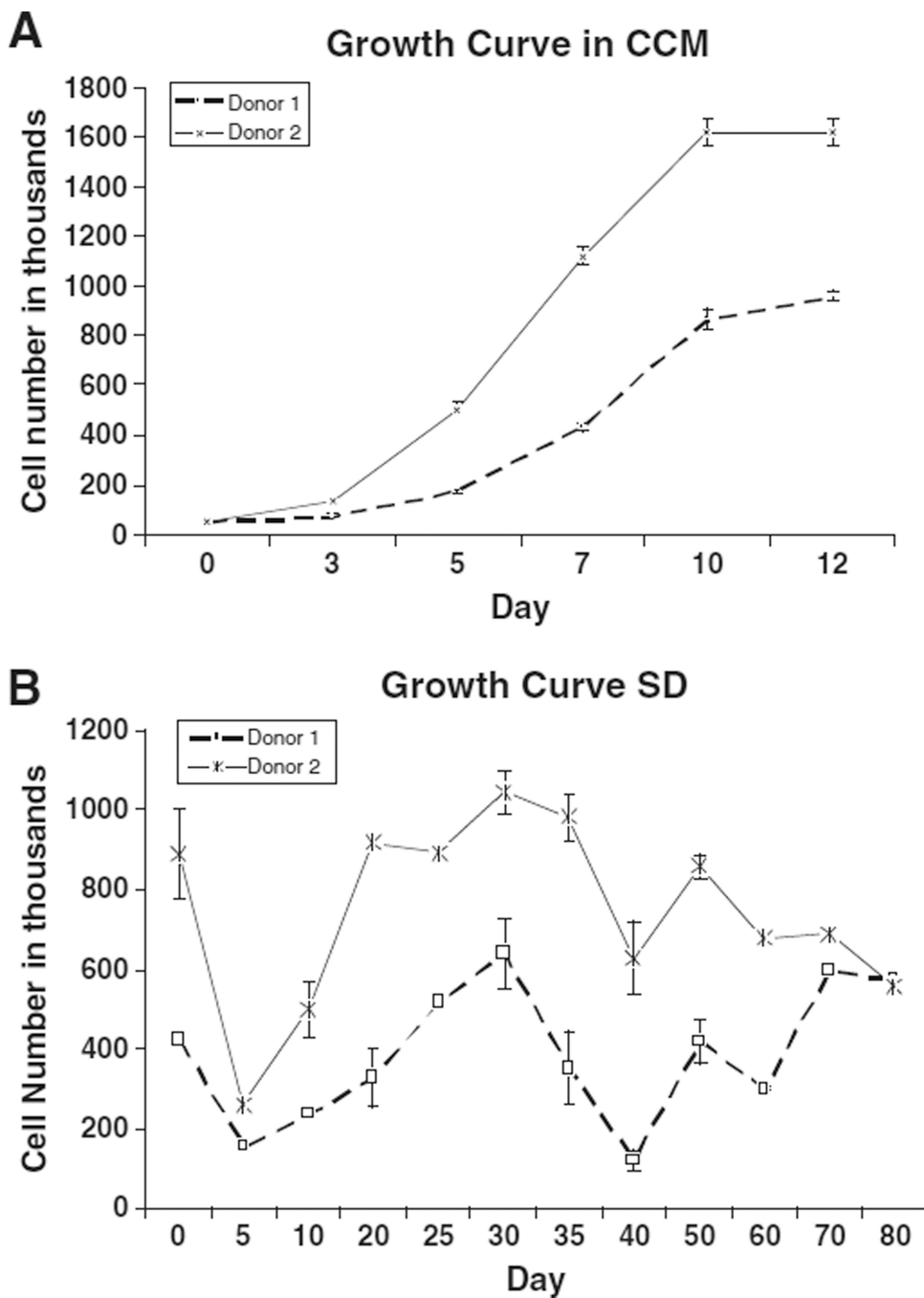


**Figure 1.** SD-MSCs continue to proliferate and secrete proteins under serum-free conditions: (A) Time course study of MSC growth in media containing 17% serum (CCM) and in serum-free media (SF). The average of 3 culture replicates is shown with SD. (B) Immunoblot of culture media conditioned by SD-MSCs on Day 30 of serum deprivation.

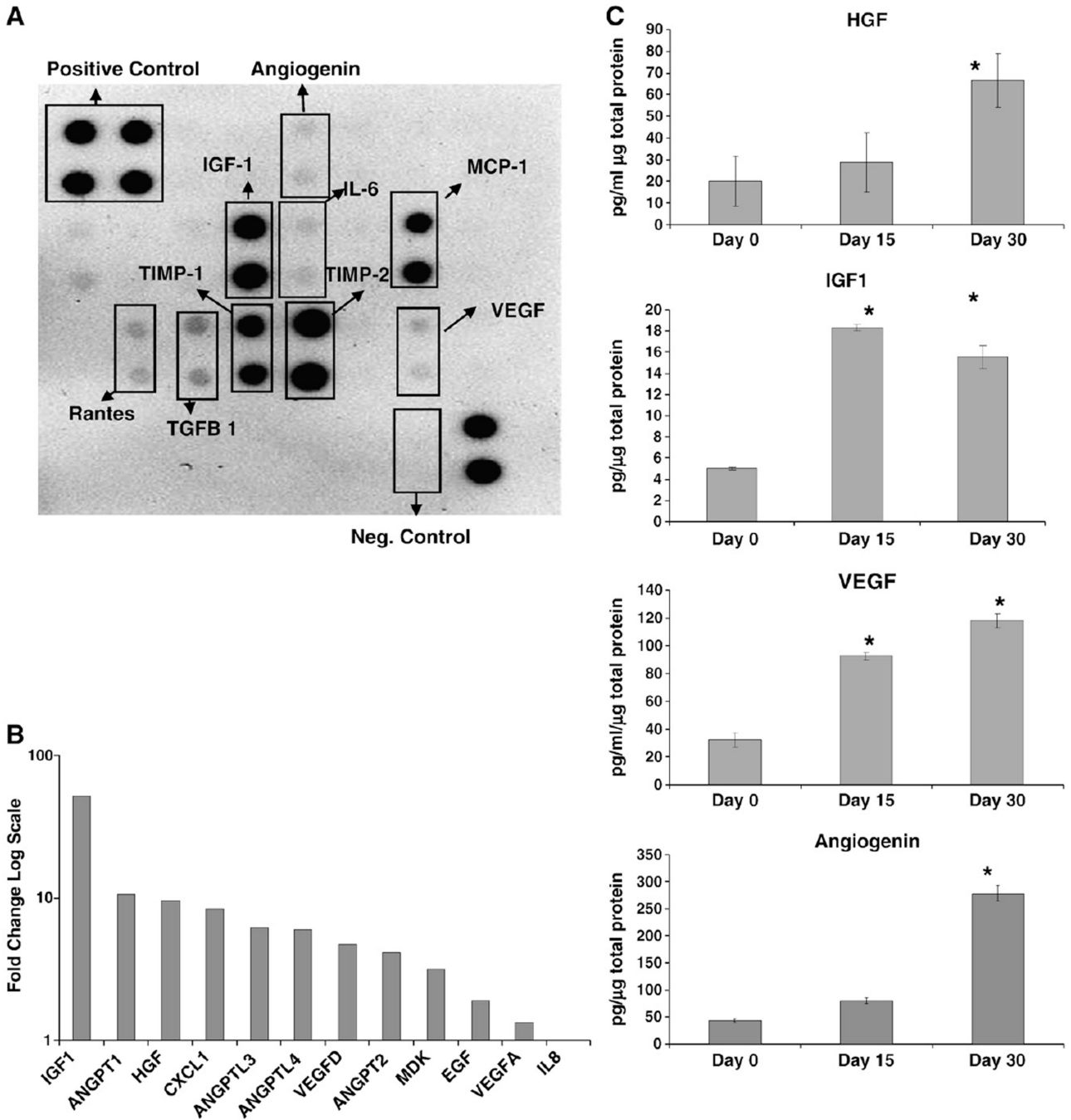


**Figure 2.** SD-MSCs express angiogenic factors: (A) Immunoblot of culture media conditioned by SD-MSCs on Day 30 of serum deprivation. (B) Relative expression of mRNA of secreted angiogenic factors in SD-MSCs from Day 30 of serum deprivation compared to donor-matched MSCs, as determined by real-time PCR. Fold change in transcript levels is represented on the Y axis in a log scale. (C) ELISAs of growth factors in conditioned media from MSCs (Day 0) and SD-MSCs (Day 15 and Day 30). Values below the minimum

detectable level of the assay are marked with a #. The average of 4 culture replicates with SD is shown. \* indicates a significant difference from Day 0 values ( $P < 0.01$ ).

Author Manuscript

Author Manuscript

Author Manuscript

Author Manuscript

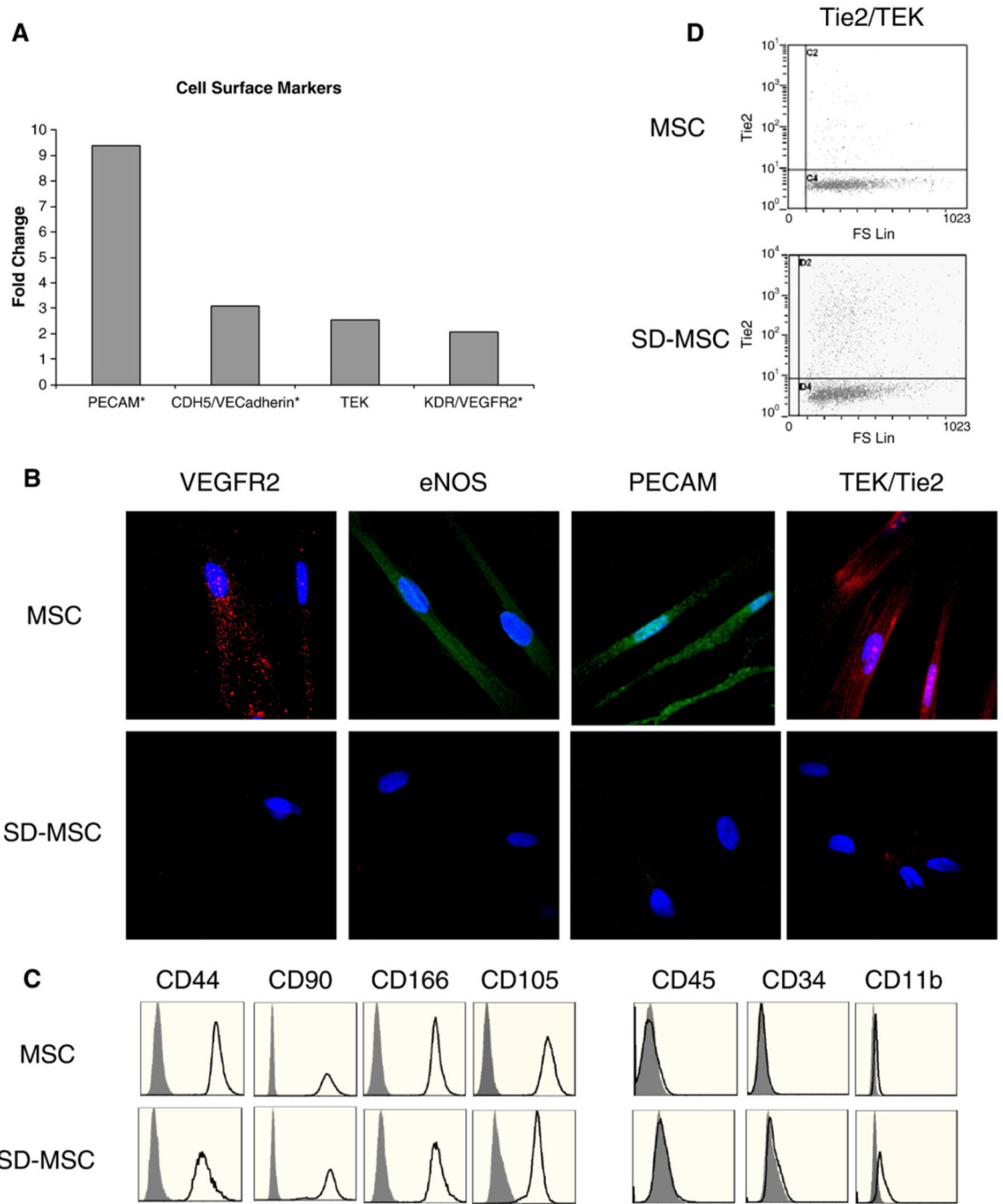


**Figure 3.** SD-MSCs express both endothelial and mesenchymal markers. (A) Relative expression of mRNA for endothelial markers in SD-MSCs on Day 30 of serum deprivation compared to MSCs. Samples below the threshold of detection are marked with a #, with fold change calculated from the lowest detectable level of mRNA. (B) Immunofluorescent images of MSCs and SD-MSCs. Samples are counterstained with DAPI (blue). Original magnification, 600 $\times$ . (C) Flow cytometric analysis of cell surface proteins of MSCs and SD-MSCs on Day 30 of serum deprivation. Open areas represent specified epitopes, gray areas represent

isotype controls. Histograms demonstrate event number ( $y$  axis) vs fluorescent intensity ( $x$  axis). (D) Flow cytometric analysis of Tie2/TEK for MSCs and SD-MSCs on Day 30 of serum deprivation. A scatter plot of fluorescent intensity ( $y$  axis) vs forward scatter is shown.

Author Manuscript

Author Manuscript

Author Manuscript

Author Manuscript

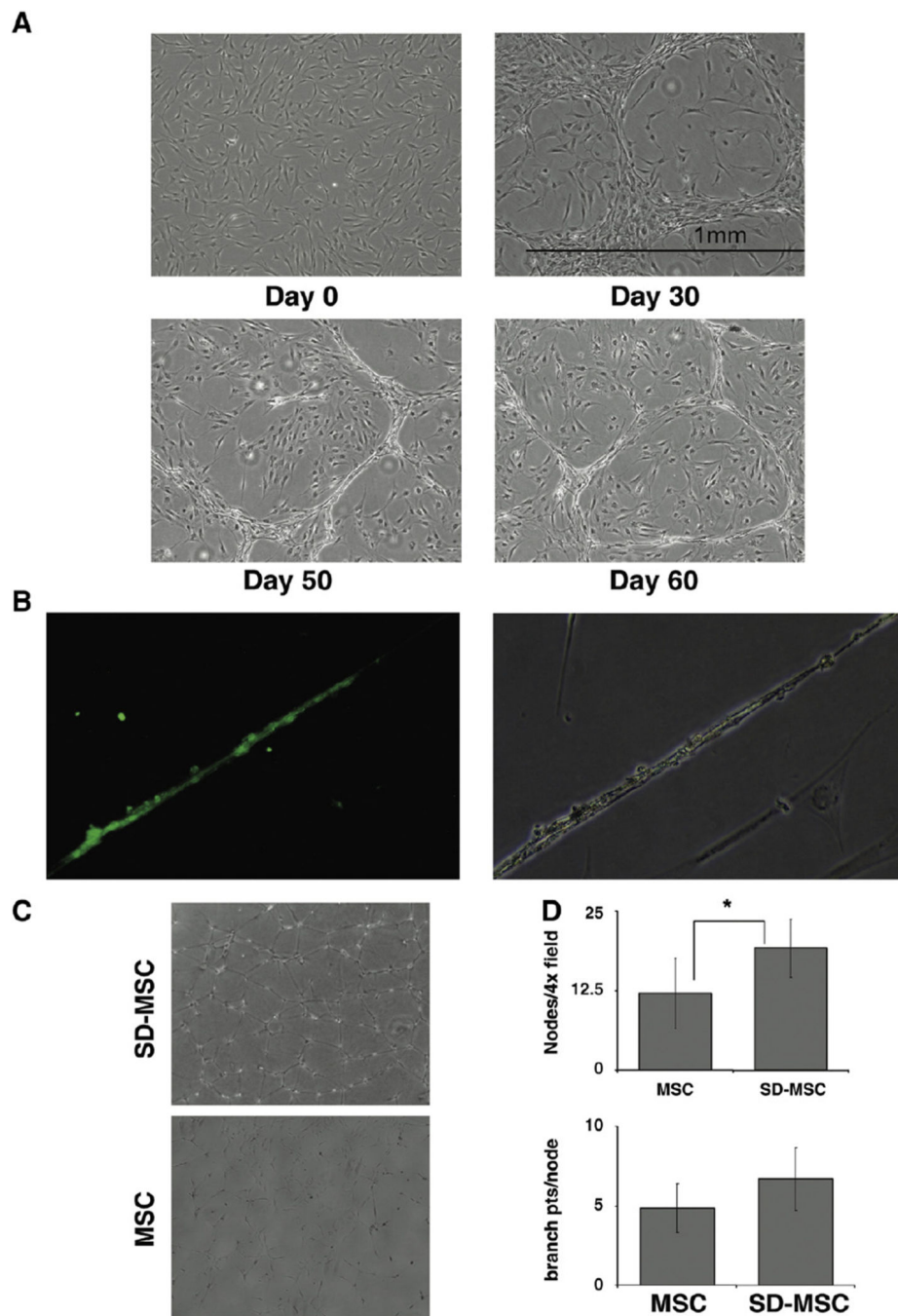


**Figure 4.** SD-MSCs exhibit endothelial cell phenotype. (A) Time course of tubule formation by MSCs cultured under serum-free conditions. Original magnification 40 $\times$ . (B) Uptake of FITC (green) labeled acLDL. SD-MSCs forming tubules on Day 30 of serum deprivation take up acLDL labeled with FITC. There is no uptake of acLDL labeled with FITC by SD-MSCs with spindle morphology. Original magnification 200 $\times$ . (C) Representative images of SD-MSCs from Day 30 of serum deprivation and MSCs after 24 h on grBME. Original magnification 100 $\times$ . (D) Quantitation of branch points and tubule pattern from cells cultured



on grBME for 24 h. The average of 8 culture replicates with SD is shown. \* indicates a significant difference from Day 0 values ( $P < 0.05$ ).

Author Manuscript

Author Manuscript

Author Manuscript

Author Manuscript

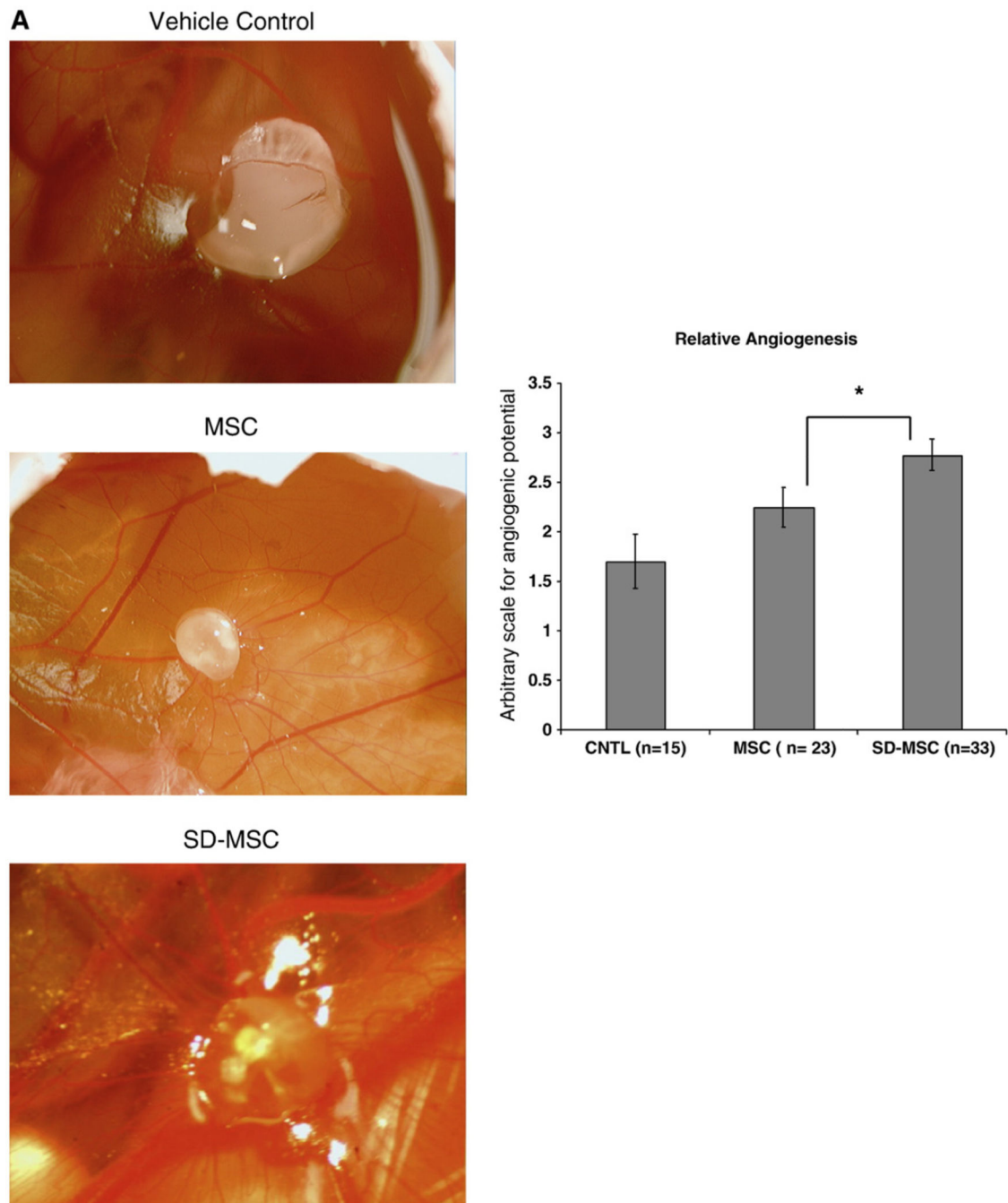
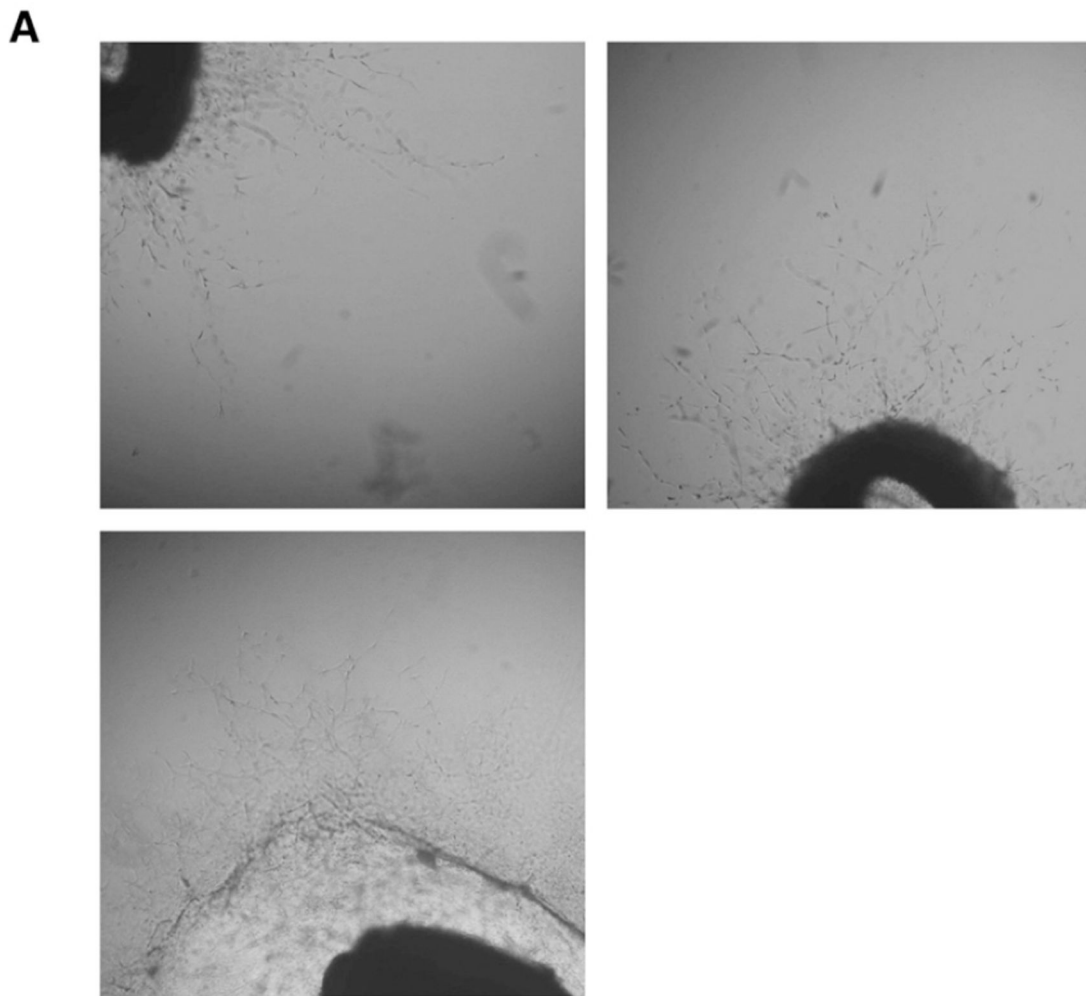


**Figure 5.** SD-MSCs are highly angiogenic *in vivo*. (A) Representative images of angiogenesis stimulated by MSCs, SD-MSCs from Day 30 of serum deprivation grown or vehicle control preincubated on grBME and placed on a developing chick CAM for 7 days. Vehicle control is grBME without cells. (B) Angiogenic level of grBME-containing cells and control rated on a 0–4 scale. The average of at least 15 samples, as judged by 2 blinded investigators, is displayed with SD. \*  $P < 0.05$ , \*\*  $P < 0.005$ .



**B**

Media	Difference From Control (microns)	Dunnet 95% CI
Day 0	192.435	17.672 to 367.197
Day 15	410.249	235.486 to 585.012

**Figure 6.**

(A) Representative images of vascular sprouts from rat aortic rings cultured in SF-CCM (control), conditioned media from MSCs (Day 0) or conditioned media from SD-MSCs (Day 15). All media were supplemented with 1% FCS. Original magnification 40 $\times$ . (B) Difference in length of vascular sprouts between samples cultured with Day 0 or Day 15 media and control. Data were generated from 110 measurements of vascular sprouts from 6 culture replicates. Data were normalized for baseline vascular sprouting by comparing

samples to a vehicle control group. The difference between measurement averages from SD-  
MSCs (Day 15) and vehicle control or MSCs (Day 0) and vehicle control are displayed.

Author Manuscript

Author Manuscript

Author Manuscript

Author Manuscript

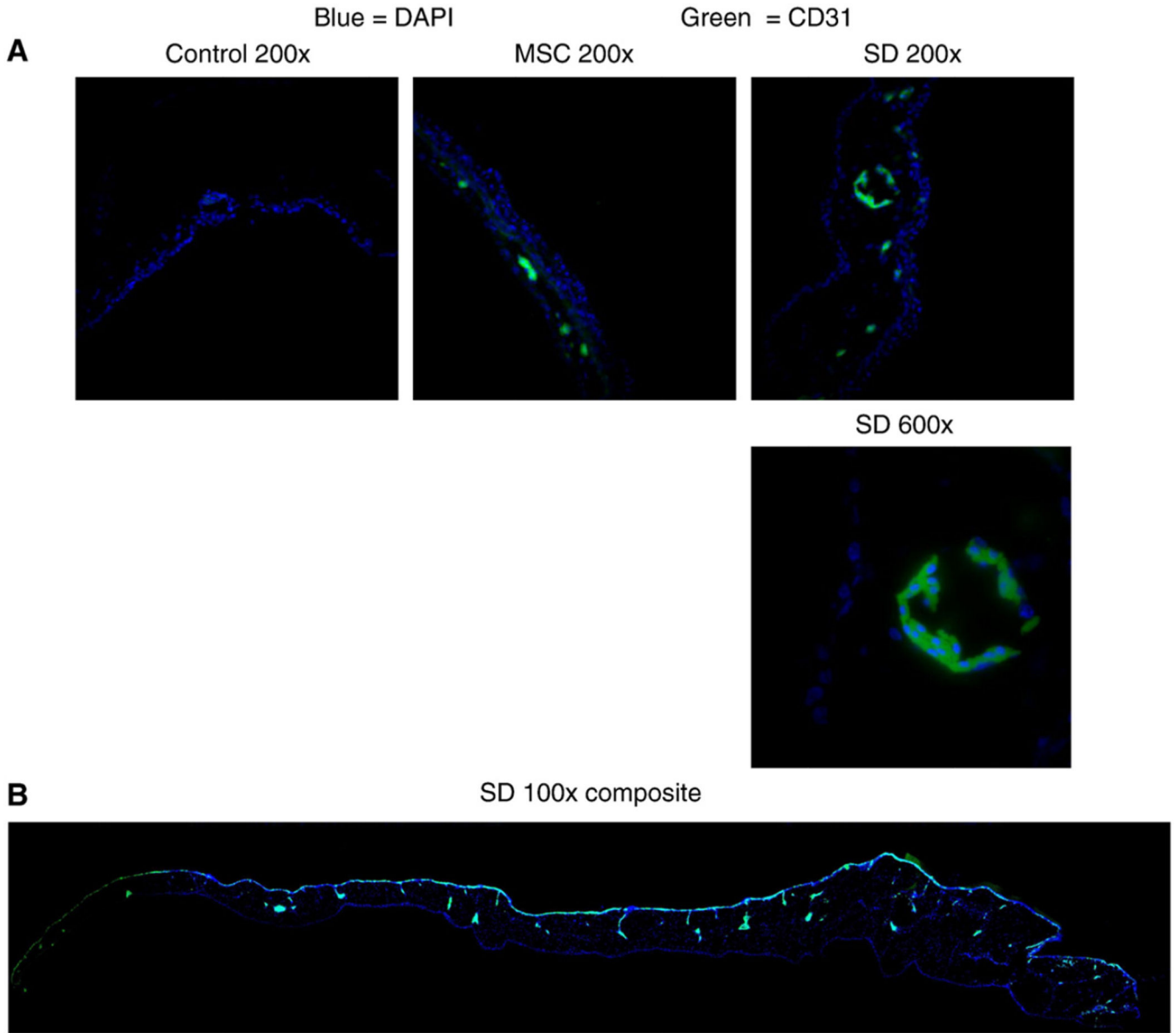


**Figure 7.** SD-MSCs express CD31 *in vivo*. (A) Representative immunofluorescent images of chick CAMs after growth with grBME-containing MSCs, SD-MSCs on Day 30 of serum deprivation, or vehicle control. Merged color images are displayed for SD-MSCs (SD), MSCs, and a vehicle control. (B) Composite image of chick CAM grown with SD-MSCs is also shown. Multiple images were taken at a magnification of 100× and then combined to create an image displaying the entire CAM. Green represents staining with a human specific CD31 antibody and blue represents DAPI staining.

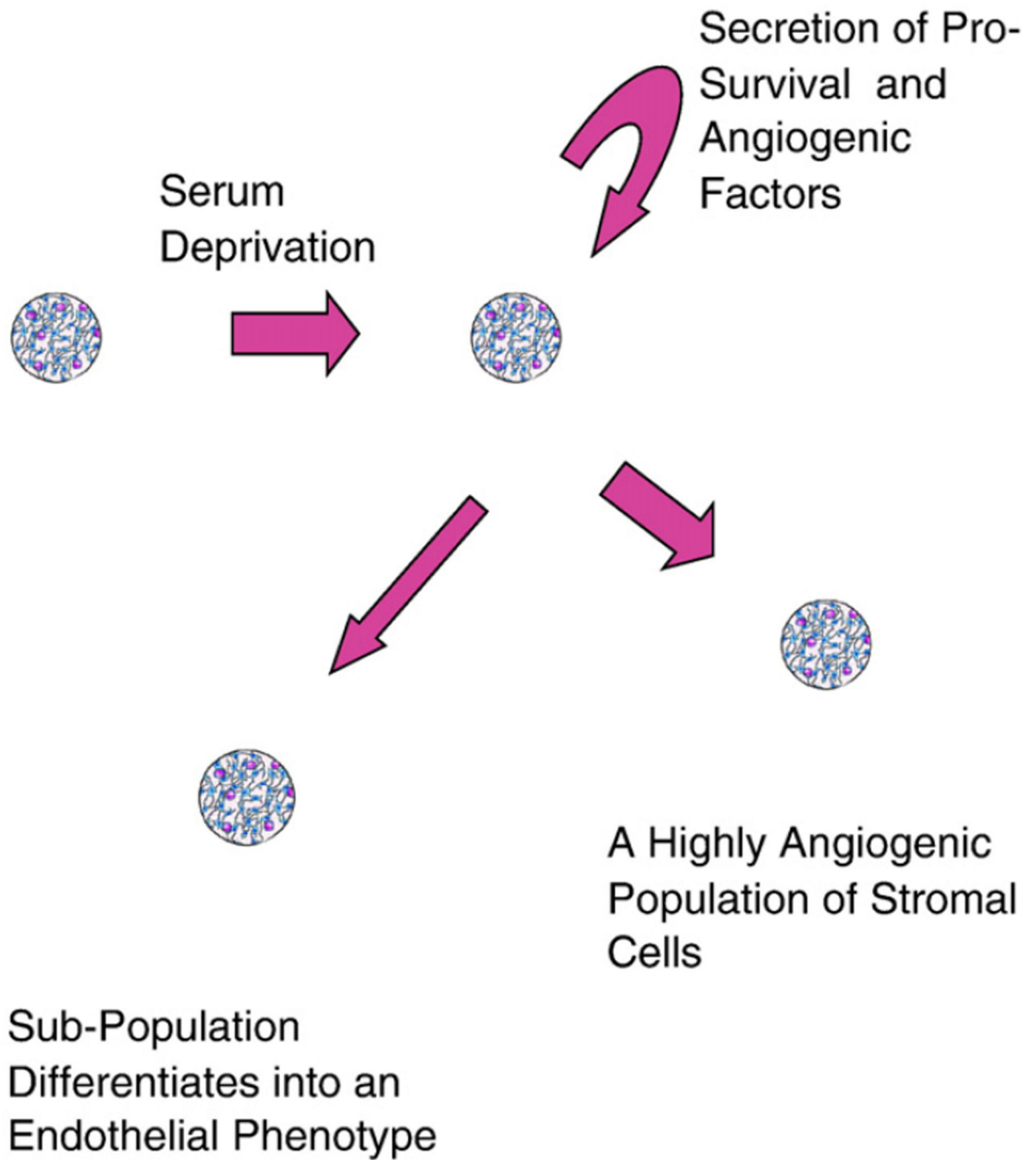


**Figure 8.**  
Representative cartoon to show angiogenic properties of SD-MSCs.